Research on the transverse mode competition in a Yb-doped 18-core photonic crystal fiber laser*

WANG Yuan(王远)[1,2]**, YAO Jian-quan**(姚建铨)[1], **ZHENG Yi-bo**(郑一博)[1,2], **WEN Wu-qi**(温午麒)[1], **LU Ying**(陆颖)[1], **and WANG Peng**(王鹏)[1]

1. *Key Laboratory on Optoelectronics Information and Technical Science, Ministry of Education of China, Institute of Laser & Optoelectronics, College of Precision Instruments and Optoelectronic Engineering, Tianjin University, Tianjin 300072, China*
2. *Hebei Key Laboratory of Optoelectronic Information and Geo-detection Technology, Shijiazhuang University of Economics, Shijiazhuang 050031, China*

(Received 27 June 2012)

A model based on propagation rate equations is built up for analyzing the multicore transverse mode gain distribution in an 18-core photonic crystal fiber (PCF) laser. The two kinds of feedback cavities are used for the fiber laser, which are the butt-contact mirror and the Talbot cavity. According to the model, the transverse mode competitions in different feedback cavities are simulated numerically. The results show that the Talbot cavity can improve in-phase supermode gain, while suppress other supermodes.

Document code: A **Article ID:** 1673-1905(2012)06-0426-4

DOI 10.1007/s11801-012-2258-x

Rare-earth-doped fiber lasers are widely used in many industries because of their high-efficiency and excellent beam quality compared with the traditional solid-state lasers. Recently kilowatt class fiber lasers with single transverse mode have been presented[1-3]. However, various nonlinear effects in fiber, such as stimulated Brillouin and Raman scattering, limit the fiber lasers to increase power further[4]. Multicore fiber lasers have an advantage of large mode areas with high doping concentration, resulting in higher power thresholds for nonlinear processes. Because of distributed nature of the cores, thermal mechanical effects of multicore fiber laser are mitigated compared with those of single-core fiber lasers[5]. Compared with multicore fiber, multicore photonic crystal fiber (PCF) can be designed for larger mode area because of its endless single-mode property[6-10]. In-phase supermode locking techniques in multicore PCF lasers, such as Talbot cavity, are discussed for improving beam quality and increasing output power[11-16]. However, analyses of transverse mode competition among various supermodes in the multicore PCF laser with Talbot cavity have not been reported. In this paper, an 18-core PCF laser is researched. Supermode distributions of the PCF are given by using full-vector finite-element method (FEM)[17]. The corresponding far field patterns of supermodes are also presented by using Fresnel diffraction integral[18]. The in-phase supermode selection based on Talbot effect is discussed. The propagation rate equations with multicore PCF are built up for simulating and calculating the competition among different supermodes.

The cross section of the 18-core PCF is shown in Fig.1. Numerical aperture (NA) of the core is about 0.04, and radius of that is 8 μm. The air-hole radius is 4.1 μm, and air-hole pitch is 10.1 μm. The inner cladding radius is about 126 μm. Each core with these parameters above only supports a single mode propagation in the PCF. By mean of FEM, mode field distribution and effective propagation constant of 18 supermodes are obtained. Fig.2 shows several patterns of supermodes. The supermodes are numbered in increasing order of their propagation constants. Fig.2(a) is the out-of-phase supermode in which phase is reverse between arbitrary adjacent cores. Fig.2(b) is the supermode in which the first and second rings are out of phase. The last mode as shown in Fig. 2(c) is the in-phase supermode in which phase is equal for every core. According to the supermode calculation, the intensity distributions at various propagation distances can be

* This work has been supported by the National Basic Research Program of China (No.2010CB327801), the Key Program of National Natural Science Foundation of China (No.60637010).

** E-mail: sjz_wangyuan@163.com

given by Fresnel diffraction integral. The far field (z=1 cm) intensity distributions of several supermodes based on Fresnel diffraction integral are also shown in Fig.2. It is shown that the in-phase supermode provides the best beam quality with a nearly Gaussian far field, whereas the out-of-phase supermode has the largest diffraction angle in the far field. For selecting the in-phase supermode, a mirror is placed at the right side to set up the Talbot cavity, which is shown in Fig. 3(b).

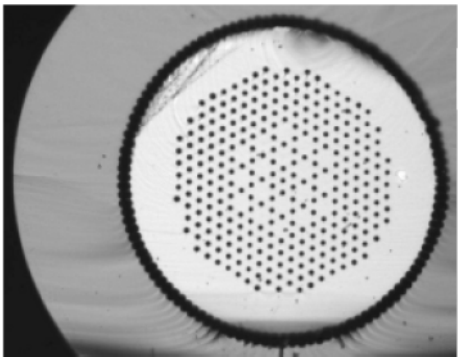

Fig.1 SEM image of the 18-core PCF

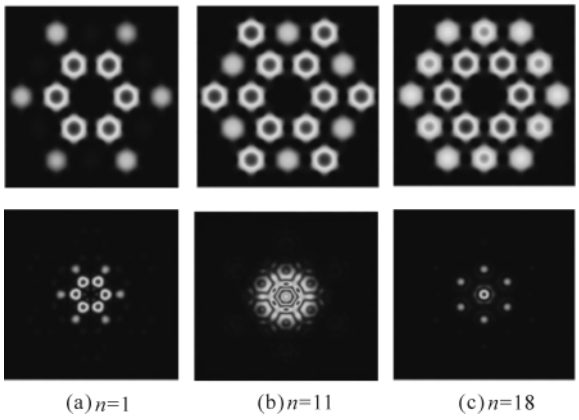

Fig.2 Some supermodes and corresponding far field (z=1 cm) intensity distributions of the 18-core fiber

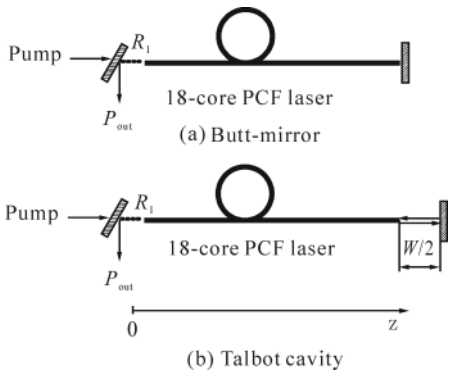

Fig.3 Two kinds of laser setup structures

For evaluating the effect of the Talbot cavity, a coupling coefficient γ is given by[19,20]

$$\gamma_{i,j}(W)=\frac{\left|\iint_{\infty}E_i^*(W=0)E_j(W)\,\mathrm{d}x\,\mathrm{d}y\right|}{\iint_{\infty}\left|E_i(W=0)\right|^2\,\mathrm{d}x\,\mathrm{d}y}\ , \tag{1}$$

where $E_i(W=0)$ and $E_j(W)$ represent the ith supermode of emitted field and the jth supermode of reflected field, respectively. W is the double Talbot distance. The self-coupling coefficients (γ_{ii}) with varying distance are shown in Fig.4, which demonstrates that self-coupling coefficients of in-phase supermode are larger than others in the range of $W/2 \geqslant 2$ mm. The in-phase supermode can be selected from other supermodes by placing a mirror at a long distance.

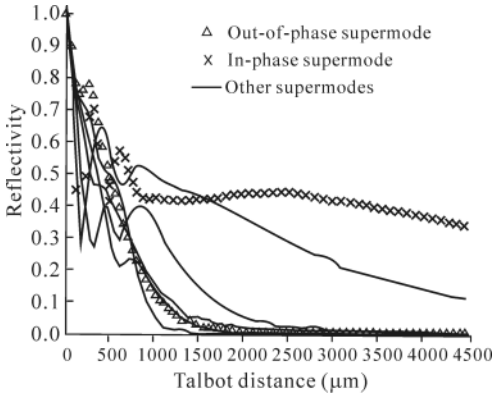

Fig.4 Self-coupling coefficient of each supermode

The 18 supermodes propagate along the fiber length and compete with each other by sharing the population inversion. Assuming that all supermodes propagate in the Yb-doped fiber, based on the propagation rate equations for ion populations in each core, we can write the equation as follows[20]:

$$N_{2j}(z)=N\times\frac{\dfrac{\Gamma_{\mathrm{p}}\sigma_{\mathrm{ap}}[P_{\mathrm{p}}^{+}(z)+P_{\mathrm{p}}^{-}(z)]}{A_{\mathrm{co}}h\nu_{\mathrm{p}}}+\sum_i\dfrac{\Gamma_{ij}\sigma_{\mathrm{as}}[P_{si}^{+}(z)+P_{si}^{-}(z)]}{A_{\mathrm{co}}h\nu_{\mathrm{s}}}}{\dfrac{\Gamma_{\mathrm{p}}(\sigma_{\mathrm{ap}}+\sigma_{\mathrm{ep}})[P_{\mathrm{p}}^{+}(z)+P_{\mathrm{p}}^{-}(z)]}{A_{\mathrm{co}}h\nu_{\mathrm{p}}}+\dfrac{1}{\tau}+\sum_i\dfrac{\Gamma_{ij}(\sigma_{\mathrm{as}}+\sigma_{\mathrm{es}})[P_{si}^{+}(z)+P_{si}^{-}(z)]}{A_{\mathrm{co}}h\nu_{\mathrm{s}}}}\ , \tag{2}$$

$$\pm\frac{\mathrm{d}P_{\mathrm{p}}^{\pm}(z)}{\mathrm{d}z}=\{\sum_j\Gamma_{\mathrm{p}}[(\sigma_{\mathrm{ap}}+\sigma_{\mathrm{ep}})N_{2j}(z)-\sigma_{\mathrm{ap}}N]-\alpha_{\mathrm{p}}\}P_{\mathrm{p}}^{\pm}\ , \tag{3}$$

$$\pm\frac{\mathrm{d}P_{si}^{\pm}(z)}{\mathrm{d}z}=\{\sum_j\Gamma_{ij}[(\sigma_{\mathrm{as}}+\sigma_{\mathrm{es}})N_{2j}(z)-\sigma_{\mathrm{as}}N]-\alpha_{\mathrm{s}}\}P_{si}^{\pm}\ , \tag{4}$$

where $N_j(z)$ is population density of upper level in the jth core, N is Yb-doping concentration (assuming that all cores have the same doping density), $P_{\mathrm{p}}^{+}(z)$ and $P_{\mathrm{p}}^{-}(z)$ are pump power in two directions, $P_{si}^{+}(z)$ and $P_{si}^{-}(z)$ are the signal power of the ith supermode in two directions, $\Gamma_{\mathrm{p}}=A_{\mathrm{co}}/A_{\mathrm{cl}}$, where A_{co} is individual core area and A_{cl} is inner cladding

area, σ_{ap} (σ_{ep}) and σ_{as} (σ_{es}) are the absorption (emission) cross-sections of pump and laser, respectively, h is the Planck constant, v_p and v_s are the pump and laser frequencies, and α_s and α_p are the loss factors of laser and pump.

The boundary conditions of the laser cavity are given by

$$P_{si}^{+}(0) = R_1 P_{si}^{-}(0) \quad , \tag{5}$$

$$P_{si}^{-}(L) = \sum_j R_{ij} P_{sj}^{+}(L) \quad , \tag{6}$$

where L is the fiber length, R_1 is the reflectivity of the reflected light to signal light, and R_{ij} is defined as the power coupling factor from the jth to the ith supermode, i.e., $R_{ij} = \gamma_{ij}^2$. The total output laser power is given by $P_{out} = \sum_i (1-R_1) P_{si}^{-}(0)$. At the beginning of the simulation, laser power of each supermode is given by an initial guess. Rate equation Eqs.(2)-(4) are iterated with the boundary conditions Eqs.(5) and (6).

Based on the discussion presented above, we simulate the behaviors of transverse supermodes competition in the 18-core Yb-doped PCF laser under two feedback methods of butt-mirror and Talbot cavity. Assume that the pump power is 100 W and R_1 is 0.035. The parameters employed in the numerical simulations are listed in Tab.1[21].

Tab.1 Parameters of 18-core Yb-doped PCF laser used in simulations

Parameter	Value	Parameter	Value
λ_p (nm)	976	L (m^{-1})	5
λ_s (nm)	1080	Γ_p	5.4×10^{-4}
σ_{ap} (m^{-2})	2.0×10^{-24}	α_s (m^{-1})	5×10^{-3}
σ_{ep} (m^{-2})	1.99×10^{-24}	α_p (m^{-1})	5×10^{-3}
σ_{as} (m^{-2})	3×10^{-27}	N (m^{-3})	5×10^{25}
σ_{es} (m^{-2})	4×10^{-25}	τ (s^{-1})	1×10^{-3}

Firstly, by using this model, we simulate the power propagation of each supermode in the 18-core PCF laser with butt-mirror as shown in Fig.3(a). For the feedback mechanism, the mirror has 100% reflection to each supermode, i.e., $R_{ii} \approx 1$ and $R_{ij} \approx 0$ when $i \neq j$, because the supermodes are orthogonal at the near field. The calculated results are shown in Fig.5. The total output power is 85.3 W with the following contributions of mode 7 with 28.1 W, mode 10 with 19.0 W, mode 16 with 7.2 W and mode 18 with 30.8 W. The total output power is a mix of four modes, in which mode 18 has the most of the power. It can be seen that the quality of output beam is bad in the system with a butt-contact mirror. Some mode-discrimination mechanism has to be introduced to favor the in-phase mode.

When a Talbot cavity is used for the 18-core PCF laser as shown in Fig.3(b), the power coupling factor R_{ij} changes with varying distance between the fiber end and the mirror. We can calculate the laser power of all supermodes based on

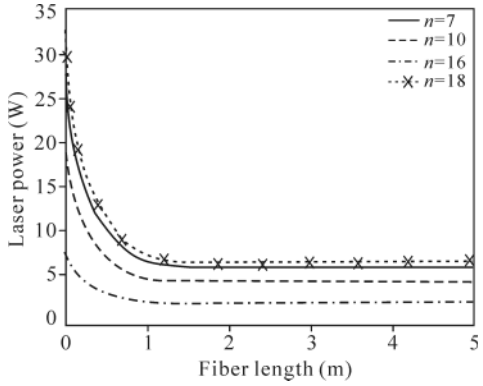

Fig.5 Laser power distribution of all supermodes along the PCF length in output direction with butt-mirror

rate equations Eqs.(2)-(4). The calculated results are shown in Fig.6. The total output power is 72.53 W and 72.20 W, respectively. It can be seen from Fig.6(b) that in-phase supermode dominates the main part of total power (about 93%), and the supermode of n=11 is about 6%.

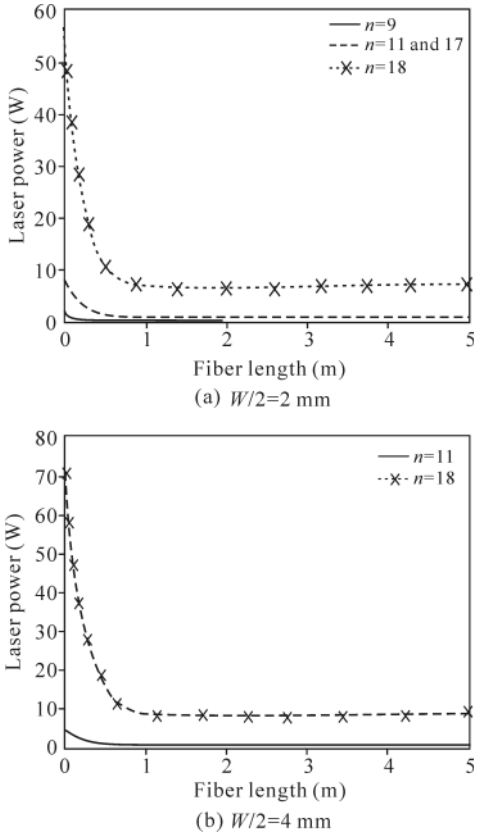

Fig.6 Laser power distribution of all supermodes along the PCF length in output direction with Talbot distance of *W*/2 = 2 mm and 4 mm, respectively

In this paper, the transverse supermode competition of an 18-core PCF laser is analyzed based on propagation rate equations extended to multicore PCF. The near field intensity distributions of all supermodes are calculated based on

FEM firstly. The Talbot cavity is used for in-phase supermode selection. The result shows that in-phase supermode is completely distinguished from the other supermodes at a long distance, and occupies a dominant position in transverse supermode competition.

References

[1] Y. Jeong, J. K. Sahu, D. N. Payne and J. Nilsson, Electron. Lett. **40**, 470 (2004).

[2] Y. Jeong, J. K. Sahu, D. N. Payne and J. Nilsson, Opt. Express **12**, 6088 (2004).

[3] A. Liem, J. Limpert, H. Zellmer, A. Tünnermann, V. Reichel, K. Morl, S. Jetschke, S. Unger, H.-P. Muller, J. Kirchhof, T. Sandrock and A. Harschak, 1.3 kW Yb-doped Fiber Laser with Excellent Beam Quality, Proc. Conference on Lasers and Electro-Optics, San Francisco, 2004.

[4] A. Babushkin, N. S. Platonov and V. P. Gapontsev, Proc. SPIE **5709**, 98 (2005).

[5] Yanming Huo and Peter K. Cheo, IEEE Photon. Technol. Lett. **16**, 759 (2004).

[6] WANG Ruo-qi, YAO Jian-quan, ZHOU Rui, WANG Jing-li, LI Jing-hui, WEN Wu-qi, LU Ying, ZHONG Kai, WEN Qi-ye and ZHANG Huai-wu, Journal of Optoelectronics • Laser **22**, 1609 (2011). (in Chinese)

[7] Kunimasa Saitob, Yukihiro Tsuchida and Masanori Koshiba, Opt, Express **13**,10833 (2005).

[8] P. St. J. Russell, J. Lightw. Techol. **24**, 4729 (2006).

[9] K. P. Hansen, C. B. Olausson, J. Broeng, K. Mattsson, M. D. Nielsen, T. Nikolajsen, P. M. W. Skovgaard, M. H. Sφrensen, M. Denninger, C. Jakobsen and H. R. Simonsen, Proc. SPIE **6873**, 687307 (2008).

[10] Shailendra K. Varshney, Kunimasa Saitoh, Ravindra K. Sinha and Masanori Koshiba, J. Lightw. Technol. **27**, 2062 (2009).

[11] D. Dorosz, M. Kochanowicz and J. Dorosz, Acta Physics Polonica A **116**, 3 (2009).

[12] Laurent Michaille, Charlotte R. Bennett, David M. Taylor and Terence J. Shepherd, IEEE J. Sel. Top. Quant. **15**, 328 (2009).

[13] Xiao-Hui Fang, Ming-Lie Hu, Yan-Feng Li, Lu Chai, Ching-Yue Wang and Aleksei M. Zheltikov, Opt. Lett. **35**, 493 (2010).

[14] Fang XiaoHui, Hu MingLie, Li YanFeng, Chai Lu and Wang QingYue, Chinese Sci. Bull. **55**, 1864 (2010).

[15] Chunying Guan, Libo Yuan and Jinhui Shi, Opt. Comm. **283**, 2686 (2010).

[16] Xiaolei Zhang, Xingyu Zhang, Qingpu Wang, Jun Chang and Gangding Peng, J. Opt. Soc. Am. A **28**, 924 (2011).

[17] ZHANG Shan-shan, ZHANG Wei-gang, LIU Zhuo-lin and LI Xiao-lan, Journal of Optoelectronics • Laser **22**, 685 (2011). (in Chinese)

[18] Yufeng Li and Turan Erdogan, Opt. Comm. **183**, 377 (2000).

[19] M. Wrage, P. Glas, D. Fisher, M. Leitner, D. V. Vysotsky and A. P. Napartovich, Opt. Lett. **25**, 1436 (2000).

[20] Yanming Huo and Peter K. Cheo, J. Opt. Soc. Am. B **22**, 2345 (2005).

[21] R. Paschotta, J. Nilsson, A. C. Tropper and D. C. Hanna, IEEE J. Quantum Electron. **33**, 1049 (1997).